



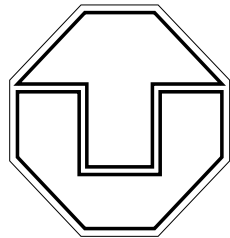
# SFB 609

Sonderforschungsbereich 609  
Elektromagnetische Strömungsbeeinflussung in  
Metallurgie, Kristallzuchtung und Elektrochemie

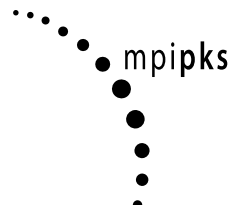
M. Hinze

**Control of weakly conductive  
fluids by near wall Lorentz forces**

SFB-Preprint SFB609-19-2004



TECHNISCHE  
UNIVERSITÄT  
DRESDEN



Preprint Reihe  
SFB 609

Diese Arbeit ist mit Unterstützung des von der Deutschen Forschungsgemeinschaft getragenen Sonderforschungsbereiches 609 entstanden und als Manuskript vervielfältigt worden.

Dresden, Juli 2005 (revidierte Version)

The list of preprints of the Sonderforschungsbereich 609 is available at:  
<http://www.tu-dresden.de/sfb609/pub.html>

# Control of weakly conductive fluids by near wall Lorentz forces

M. Hinze\*<sup>1</sup>

<sup>1</sup> TU Dresden, Institut für Numerische Mathematik, Zellescher Weg 12–14. 01062 Dresden

Received 22 July 2005

Published online 22 July 2005

**Key words** Weakly conductive fluids, Navier-Stokes equations, optimal control, model-predictive control.

**MSC (2000)** 00-xx

In this work optimal and model-predictive control approaches for control of weakly conductive fluids are developed. The flow around the circular cylinder at low Reynolds numbers serves as prototyping application. Control by near-wall Lorentz forces gains either to suppress the formation of the von Kármán Vortex Street, or to reduce the drag. Besides a coincide mathematical modelling numerical examples are presented which highlight the scope of the presented control approaches.

Copyright line will be provided by the publisher

## 1 Introduction

Flow over a bluff body induces drag and lift forces which are undesriable. During the past 100 years there have been many experimental approaches to control the flow around a bluff body in order to reduce drag and increase lift forces and suppress separation, e.g. with shaping, blowing/suction, splitter plates, secondary objects and rotation. A comprehensive review can be found in e.g. [5].

In the recent past methods from magneto-hydrodynamics (mhd) have become a more and more acknowledged in control of conductive fluids by Lorentz forces cf. [6, 3, 13, 18].

In this work model-predictive and optimal control approaches for control of weakly conductive incompressible fluids are developed. The flow around the circular cylinder at low Reynolds numbers serves as prototyping application. Control by near-wall Lorentz forces gains either to suppress the formation of the von Kármán Vortex Street, or to reduce the drag.

It is well known that weakly conductive fluids like sea water and other electrolytes can be controlled by means of near wall body forces [6, 3] which exponentially decay into the fluid. In an experimental setting appropriately arranged stripes of alternating electrodes and magnets allow to generate a volumetric force called Lorentz force perpendicular to the electric and magnetic field, see Fig. 1. The Lorentz force per unit volume in an electrically conducting fluid of conductivity  $\sigma$  is given by

$$F_L = J \times B, \tag{1}$$

---

\* Corresponding author: e-mail: hinze@math.tu-dresden.de, Phone: +49 351 463 37584, Fax: +49 351 463 34268

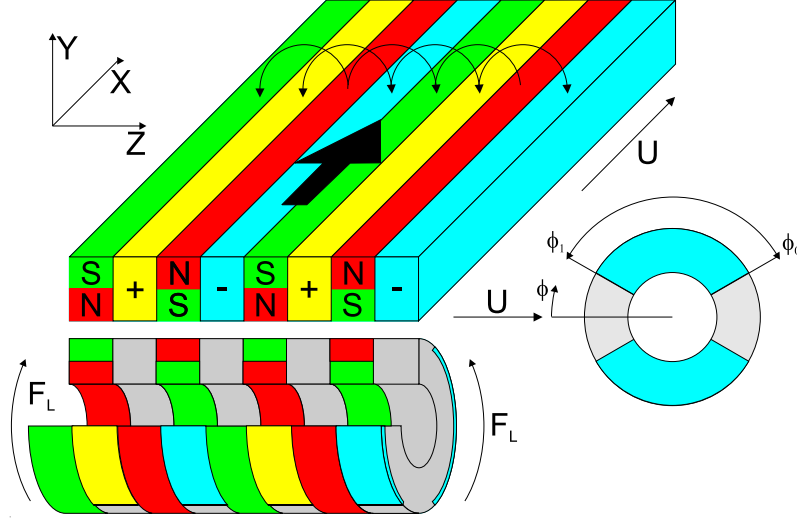


**Fig. 1** Actuator configuration inducing a streamwise Lorentz force.

where  $J$  is the current density and  $B$  denotes the magnetic induction. Ohm's law applied to a fluid moving with free-stream velocity  $U$  has the form

$$J = \sigma (E + U \times B), \quad (2)$$

with  $E$  denoting the externally aligned electric field. The magnetic Reynolds number  $Re_m$  of a conducting fluid represents the ratio between the characteristic time for magnetic diffusion and the transit time for fluid particles. It is given by

$$Re_m = \mu \sigma U D, \quad (3)$$

with  $\mu$  denoting the magnetic permeability and  $D$  the cylinder diameter as characteristic length. In the present work it is assumed that  $\mu \approx \mu_0$  is constant and that the magnetic field induced by the flow is small compared to the applied magnetic field, so that (1) reduces to

$$J = \sigma E. \quad (4)$$

It is further assumed that the array of magnets only contains permanent magnets, so that the electric field does not depend on the magnetic field and thus, that the Lorentz force can be calculated independent of the flow. It is worth noting that for seawater the magnetic Reynolds number satisfies the relation

$$Re_m \approx 5 \cdot 10^{-12} Re, \quad (5)$$

with  $Re = \frac{UD}{\nu}$  denoting the Reynolds number, and  $\nu$  the constant kinematic viscosity.

To ensure existence and uniqueness of solutions of the Navier-Stokes system in parts of this work it is assumed that the flow is two-dimensional which in the context of wall-tangential

fbw control is also justified for higher Reynolds numbers, compare the work of Poncet and Koumoutsakos [12]. It is further assumed that the Lorentz forces decays exponentially into the fluid in wall-normal direction, compare the work of Gailitis and Lielausis [6], and the appendix of Berger et al. [3], where this fact is theoretically justified.

To the best of the author's knowledge model-predictive and optimal control techniques have not yet been applied to control weakly conducting fluids. Numerical investigations for control of the cylinder fbw with constant Lorentz forces at low Reynolds numbers are presented by Posdziech and Grundmann in [13], by Chen [1], and Chen and Aubry in [2]. Berger et al. in [3] show the effectiveness in skin-friction reduction of temporally oscillating Lorentz forces for turbulent channel fbws at low Reynolds numbers. A lot of experimental work can be found in the work of Weier et al. [15, 16, 17, 18].

The present work is organised as follows. In Section 2 mathematical modelling of optimal and model-predictive control problems for weakly conductive fluids is presented, including numerical experiments for control of the laminar cylinder fbw by near wall Lorentz forces. Section 3 presents some conclusions.

## 2 Mathematical modelling

In the present work control of weakly conductive fluids by Lorentz forces is considered. The fbw is governed by the unsteady incompressible Navier Stokes equations, and the Lorentz force  $F_L$  in this case can be modelled by a near wall distributed force [3]. The fluid fbw with external forcing  $F_L$  and initial velocity distribution  $y_0$  in the open, bounded domain  $\Omega \subset \mathbb{R}^{2,3}$  is governed by the incompressible Navier-Stokes system which in the primitive setting reads

$$\begin{aligned} y_t - \nu \Delta y + (y \nabla) y + \nabla p &= F_L & \text{in } Q := (0, T) \times \Omega, \\ -\nabla \cdot y &= 0 & \text{in } Q, \\ y(0) &= y^0 & \text{in } \Omega, \end{aligned} \quad (6)$$

supplied with appropriate boundary conditions. The Lorentz force is modelled with time dependent amplitudes  $u_j(t)$  ( $j = 1, \dots, m$ ) which serve as control variables, and exponentially decaying spatial components  $F_j(x)$  ( $j = 1, \dots, m$ ) in the following form;

$$F_L(t, x) = (Bu)(t, x) := \sum_{j=1}^m u_j(t) F_j(x). \quad (7)$$

For the numerical investigations the fbw around a circular cylinder in two space dimensions is chosen. In this case one Ansatz for the Lorentz force has the form

$$(Bu)(t, x) := u(t) g(\phi) e^{-\frac{\pi}{a} \text{dist}(x, \text{cylindersurface})} \vec{t}, \quad (8)$$

where  $t$  denotes the tangent vector on the cylinder surface,  $a$  the electrode–magnet spacing (compare Fig. 1, where an electrode/magnet arrangement is sketched which produces a tangential Lorentz force. Note, that by altering this arrangement also orthogonal near wall Lorentz forces can be generated [3]) and

$$g(\phi) = \begin{cases} 1, & \phi_0 \leq \phi \leq \phi_1 \\ -1, & \pi + \phi_0 \leq \phi \leq \pi + \phi_1 \\ 0, & \text{else.} \end{cases}$$

Thus,  $Bu$  is of the form in (7) with  $m = 1$  and  $F_1(x) = g(\phi)e^{-\frac{\pi}{\alpha} \text{dist}(x, \text{cylindersurface})} \vec{t}$ . Note that the amplitude is proportional to the interaction parameter  $N$ , whose definition can be found in e.g. [13], and that the actuation in (8) is learnt from an experimental setting [15].

## 2.1 Optimal control

The control target on the mathematical level is specified in terms of a cost functional  $J(y, p, u)$ . If for the cylinder flow the control target consists in suppressing the vortex shedding behind the cylinder (and thus implicitly minimising the drag), typical optimisation problems read

1. Given a desired state  $z$  (for which one knows that it admits the desired flow properties), find amplitudes  $u$ , the flow  $y = y(u)$  and pressure  $p = p(u)$ , such that

$$J(y, p, u) := \frac{\alpha}{2} \int_0^T \int_{\Omega} |y - z|^2 dx dt + \frac{\delta}{2} \int_{\Omega} |y(T) - z(T)|^2 dx dt + \frac{\gamma}{2} \int_0^T |u|^2 dt \quad (9)$$

is minimised.

2. Suppress backflow on the cylinder surface by minimising

$$J(y, u) := \frac{1}{4} \int_0^T \int_{\partial_{\text{cyl}}} \partial_{\eta}(y \cdot \tau) \eta_2 (|\partial_{\eta}(y \cdot \tau) \eta_2| - \partial_{\eta}(y \cdot \tau) \eta_2) dO dt + \frac{\gamma}{2} \int_0^T |u|^2 dt. \quad (10)$$

3. Reduce the drag on the cylinder surface by minimising on the cylinder surface ( $d$  diameter of the cylinder,  $\rho = 1$  fluid density,  $U$  bulk velocity):

$$J(y, p, u) := \frac{2}{\rho d \bar{U}^2} \int_0^T \int_{\partial_{\text{cyl}}} \rho \nu \partial_{\eta}(y \cdot \tau) \eta_2 - p \eta_1 dO dt + \frac{\gamma}{2} \int_0^T |u|^2 dt. \quad (11)$$

In all cases the control function and the state variables  $(y, p)$  are connected through the Navier-Stokes system (6) which models the fluid flow over the time horizon  $[0, T]$ . Note, that in many practical applications controls have to satisfy constraints. In the case considered here amplitudes may not become too large, which mathematically can be achieved by the requirement  $|u(t)| \leq \text{amax}$  for all  $t \in [0, T]$  with  $\text{amax}$  denoting some positive constant.

For two-dimensional flows it is well known that the Navier-Stokes system (6) for every right hand side  $F_L$  admits a unique solution  $(y(u), p(u))$ , so that it is meaningful to introduce the reduced cost functional

$$\hat{J}(u) = J(y(u), p(u), u). \quad (12)$$

Minimising  $J(y, p, u)$  subject to (6) and  $|u(t)| \leq \text{amax}$  then is equivalent to minimising  $\hat{J}(u)$  subject to  $|u(t)| \leq \text{amax}$ . Let us call this problem  $\mathbb{O}$ . It is well known that  $\mathbb{O}$  admit solutions

for a large class of cost functionals [11, 8, 10], including that of (9). From here onwards the constraints on the the amplitudes are neglected, i.e.  $\text{amax} := \infty$ .

To apply derivative based optimisation algorithms to the solution of  $\textcircled{O}$  it is convenient to express the first and second derivatives of  $\hat{J}$  with the help of the adjoint variables. Let us concentrate on the first derivative  $\hat{J}'(u)$  (for the characterisation of the Hessian of  $\hat{J}$  see [8, 10]), which is given by

$$\hat{J}'(u) = J_u(y(u), p(u), u) + B^* \lambda, \quad (13)$$

where  $B^*$  denotes the adjoint operator of  $B$ , and  $\lambda$  denotes the adjoint vector field. For the cost functional of (9) it together with the adjoint pressure  $\pi$  satisfies the system

$$\begin{aligned} -\lambda_t - \nu \Delta \lambda - (\lambda \nabla) y + (\nabla y)^t \lambda &= -\nabla \pi \alpha (y - z) && \text{in } Q := (0, T) \times \Omega, \\ -\nabla \cdot \lambda &= 0 && \text{in } Q, \\ \lambda(T) &= \delta(y(T) - z(T)) && \text{in } \Omega, \end{aligned} \quad (14)$$

plus boundary conditions. Here,  $y = y(u)$  denotes the fbw corresponding to the force  $Bu$ , and with  $\lambda$  available there holds

$$B^* \lambda = \left( \int_{\Omega} \lambda(t, \cdot) F_1(x) dx, \dots, \int_{\Omega} \lambda(t, \cdot) F_m(x) dx \right)^t,$$

which defines a time dependent function in  $\mathbb{R}^m$ .

With the descent direction  $d := -\hat{J}'(u)$  available every descent algorithm with descent direction  $d$  may be applied to solve the optimisation problem  $\textcircled{O}$ . It is worth noting that with  $\lambda$  available the directional derivative of the functional  $\hat{J}$  in direction  $v$  can be computed by simply forming the scalar product of  $v$  with  $\hat{J}'(u)$  from (13) in  $L^2(0, T)^m$ . Moreover, every iteration step of a descent algorithm with descent direction  $d$  amounts to solving the Navier-Stokes equations (6) for  $y(u)$  with right hand side  $Bu$ , and then the adjoint system (14) for  $\lambda$  with right hand side  $\alpha(y - z)$  and initial values  $\delta(y(T) - z(T))$ . For a further discussion of numerical approaches to control of the Navier-Stokes system see [8, 10].

### 2.1.1 Numerical experiments for optimal control

The following numerical experiments present results for control of the fbw around a circular cylinder at  $\text{Re} = \frac{UD}{\nu} = 100$ . The fbw domain is depicted in Fig. 2.1.1. The cylinder diameter is taken as  $D = 0.1$ , and at the inlet a block velocity profile is prescribed so that the bulk velocity satisfies  $U = 1$ . Thus, the viscosity in (6) is taken as  $\nu = \frac{1}{1000}$ . At the upper and lower the boundary the conditions  $y = (1, 0)^t$  are prescribed, at the outfbw boundary natural boundary conditions are taken, i.e. there holds  $\nu \partial_\eta y = p\eta$ . As initial condition  $y^0$  the fully developed wake fbw at  $\text{Re} = 100$  is taken. The time grid is equidistant with time step size  $\delta t = 0.002$ . The Lorentz force is taken as in (8) with  $\phi_0 = \frac{\pi}{18}$ ,  $\phi_1 = \frac{17\pi}{18}$  and  $a = \frac{1}{10}$ .

In Fig.2.1.1 the numerical results for the minimisation of the functional in (9) with  $z$  the Stokes fbw,  $\alpha = 0$ ,  $\gamma = \frac{1}{100}$  and  $\delta = 1$  are presented. As picture a) shows, the optimal amplitude is a periodic function of time. Picture b) presents the drag for the controlled and the uncontrolled fbw. As one can see optimal forcing with the chosen Ansatz for the Lorentz force yields a drag reduction of approximately 10% compared to the uncontrolled case.

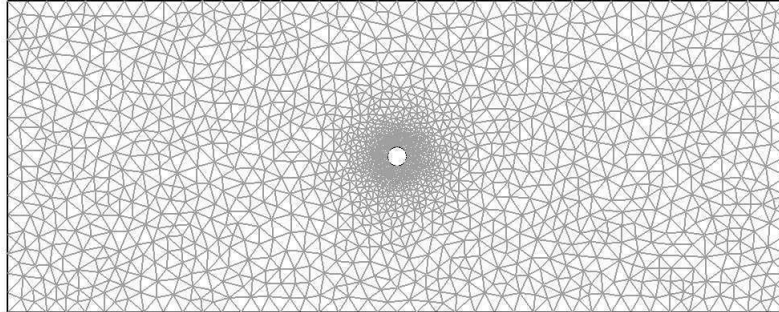


**Fig. 2** Flow domain together with computational grid

Fig.2.1.1 presents the numerical results for the parameter triple  $\alpha = 1$ ,  $\gamma = \frac{1}{100}$  and  $\delta = 10$ . Again the optimal amplitude is a periodic function of time. The dramatic increase of the amplitude at  $t \approx 3$  is caused by the large value of  $\delta$  and also results in a further drag reduction. In this connection it should be noted that the reduction of the drag is a by-product of the minimisation problem, since drag does not explicitly occur in the cost functional (9). Drag here is reduced since the total drag of the desired flow  $z$  admits a smaller value than that of the uncontrolled cylinder flow.

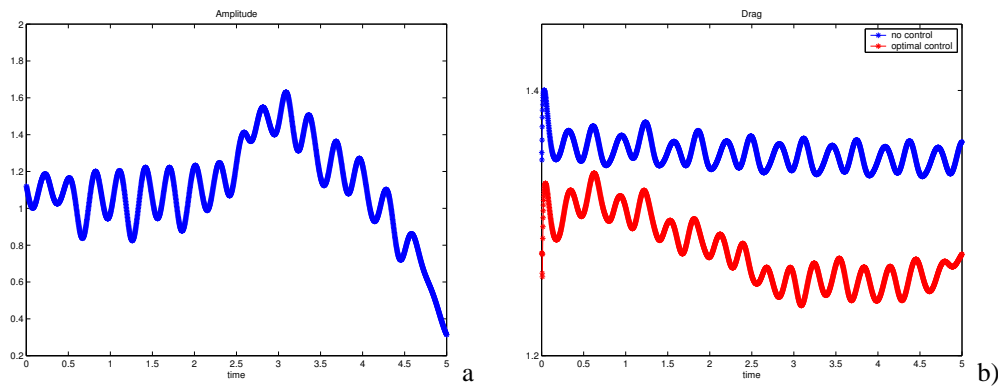


**Fig. 3** Amplitude a) and drag b) for  $\alpha = 0$ ,  $\gamma = \frac{1}{100}$  and  $\delta = 1$

## 2.2 Model predictive control

Instead of seeking for control policies on prescribed time horizons  $[0, T]$  (which is often called open-loop optimal control) one may wish to develop closed-loop control strategies, since they also offer the possibility to control the system in the presence of disturbances. A class of such strategies are the model-predictive or receding-horizon control strategies (mpc). Their key idea consists in computing discrete-in-time optimal control strategies on certain discretized control horizons and to use the first control of the strategy to steer the system to the next time instance, compare [7, 14]. An inexact variant of mpc is the so called instantaneous control

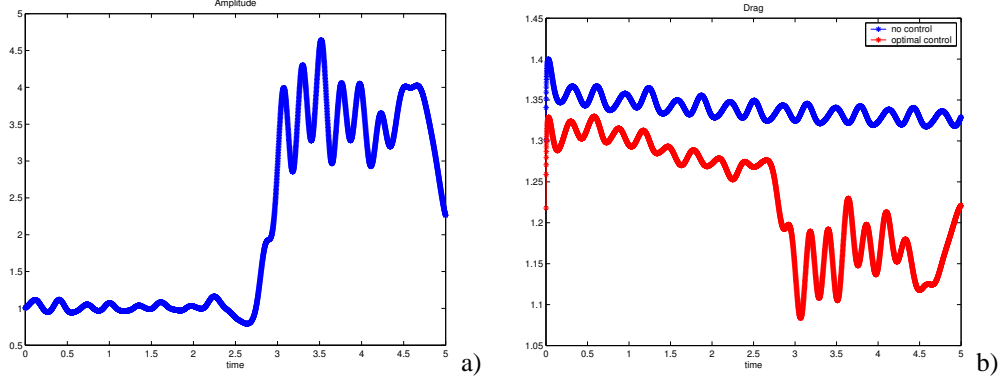


**Fig. 4** Amplitude a) and drag b) for  $\alpha = 1$ ,  $\gamma = \frac{1}{100}$  and  $\delta = 10$

strategy, see e.g. [4]. To apply it to control the cylinder flow first apply the following semi-implicit time discretization scheme with time step  $\delta t$  to the Navier-Stokes system (6): Given  $y^i, u^{i+1}$ , find  $y^{i+1}, p^{i+1}$  such that

$$e(y^{i+1}, p^{i+1}, u^{i+1}) = 0 \iff \begin{pmatrix} \frac{1}{\delta t} \text{Id} - \nu \Delta & \nabla \\ -\text{div} & 0 \end{pmatrix} \begin{pmatrix} y^{i+1} \\ p^{i+1} \end{pmatrix} = \begin{pmatrix} r^i \\ 0 \end{pmatrix}, \quad (15)$$

where  $r^i := \frac{1}{\delta t} y^i - (y^i \nabla) y^i + (Bu)^{i+1}$ ,  $y^{i+1}$  is supplied with appropriate boundary conditions,  $y^0$  denotes the initial condition and  $Bu$  the Lorentz force defined in (8). System (15) for every  $r \in L^2(\Omega)^2$  admits a unique solution  $y, p$  (superscripts are dropped), so that  $y$  and  $p$  as in the previous subsection might be considered as functions of the amplitude  $u$ . Next denote by  $J(y, p, u)$  some (now instantaneous) performance measure which allows to relate the control gain (here suppression of vortex shedding and/or drag reduction) to the state variables  $y, p$  and to the control action  $u$ .

At time instance  $t^{i+1}$  consider now the minimization problem

$$\min \hat{J}(u) := J(y(u), p(u), u) \text{ s.t. } e(y, p, u) = 0. \quad (16)$$

It is well known that the gradient of  $\hat{J}(u)$  takes the form (compare (13))

$$\hat{J}'(u) = J_u(y, p, u) - e_u^*(y, p, u)(\lambda, \xi), \quad (17)$$

where  $(\lambda, \xi)$  solves the adjoint system

$$e_y^*(y, p, u)(\lambda, \xi) = J_y(y, p, u). \quad (18)$$

Here,  $*$  denotes adjoining.

The instantaneous control strategy works now as follows. At every time instance  $t^i$ , given a control  $u_o$ , compute a new control  $u_n$  by the steepest descent method, i.e. set

$$u_n = u_o - s \hat{J}'(u_o), \quad (19)$$

where  $s > 0$  denotes the gradient step size, and apply  $u_n$  to control the system (15). Then proceed to the next time slice and repeat the process. A mathematical investigation of instantaneous control applied to flow control can be found in [9].

Let the control target consist in reducing the friction force

$$F_{D_f} = \int_{\partial\text{cyl.}} \rho\nu\partial_\eta(y \cdot \vec{t}) \cdot \eta_2 dS,$$

where  $\eta = (\eta_1, \eta_2)^t$  denotes the outward normal on the cylinder surface. A suitable cost functional then is given by

$$J(y, p, u) := \int_{\partial\text{cyl}} \rho\nu\partial_\eta(y \cdot \vec{t})\eta_2 dS + \frac{\gamma}{2}|u|^2.$$

The first term here measures the quantity of interest, the second term the control cost, where  $\gamma > 0$  plays the role of a weight. Since  $e_u = -B$  one has

$$\hat{J}'(u) = \gamma u + B^* \lambda,$$

where  $(\lambda, \xi)$  solves the adjoint equations (compare (18))

$$\begin{aligned} \frac{1}{\delta t} \lambda + \nu \Delta \lambda + \nabla \xi &= 0 && \text{in } \Omega, \\ -\operatorname{div} \lambda &= 0 && \text{in } \Omega, \\ \lambda_1 &= \eta_2^2 && \text{on } \partial\text{cyl}, \\ \lambda_2 &= -\eta_1 \eta_2 && \text{on } \partial\text{cyl}, \\ \lambda &= 0 && \text{on } \partial\Omega \setminus (\partial\text{cyl} \cup \text{outflow boundary}), \\ \nu \partial_\eta \lambda &= \xi \eta && \text{on outflow boundary,} \end{aligned}$$

and

$$B^* \lambda = \int_{\Omega} \lambda g(\phi) \vec{t} dx.$$

Note that the adjoint variable  $\lambda$  is independent of  $y$  and  $p$  and therefore can be computed a priori. The update of the control in (19) for  $s = \frac{1}{\gamma}$  (which is the optimal step size since the cost functional is linear w.r.t.  $y$  and quadratic in  $u$ ) now reads

$$u_n = \frac{\gamma - 1}{\gamma} u_a - \frac{1}{\gamma} \int_{\Omega} \lambda g(\phi) \vec{t} dx.$$

### 2.2.1 Numerical results for instantaneous control

Unless otherwise stipulated, the same data as in Subsection 2.1.1 is used. The time step in (15) is chosen as  $\delta t = 0.001$  and instantaneous control is applied on the horizon  $[0, 4]$ , i.e.  $T = 4$ , with  $u_a \equiv 0$ . The resulting Lorentz force at every time instant of course is constant, since here  $u_n = -\frac{1}{\gamma} \int_{\Omega} \lambda g(\phi) \vec{t} dx$ . This results in a different control policy than that obtained by optimal control in Subsection 2.1.1 which is a periodic function of time. The constant force

is presented in Fig. 5, b). The constant amplitude computed by the instantaneous control strategy in the present computations corresponds to an interaction parameter of  $N = 1.075$ . Fig. 5, a) shows the evolution of the drag (blue), the friction drag (green) and of the pressure drag (red). Control is switched on at  $t = 1$ . As can be seen, a drag reduction of approximately 20% is achieved. Note that the interaction parameter is not a-priori specified. It results from

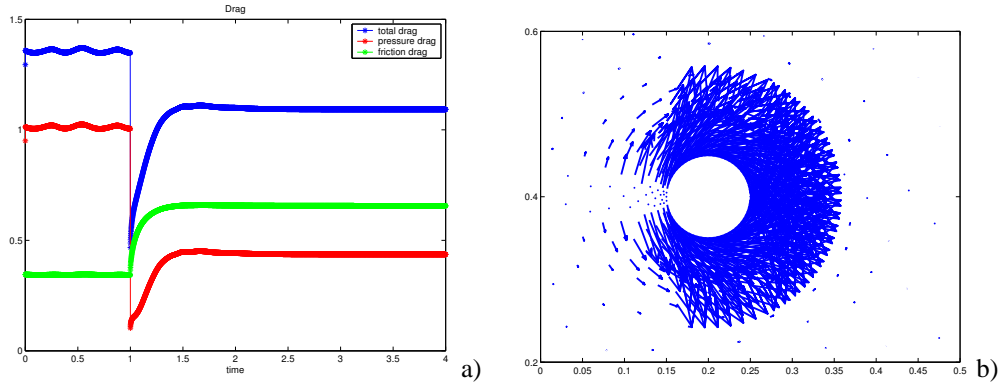


**Fig. 5** Development of drag in instantaneous control a), and constant Lorentz force resulting from instantaneous control b).

the optimisation approach.

### 3 Conclusions

Two model based optimisation approaches are presented which allow to compute near wall Lorentz forces tailored to track a prescribed flow field and/or to minimise drag. The laminar flow around an circular cylinder serves as prototyping application. The actuation in the mathematical model is learnt from an experimental setting. Open-loop optimal control for this application computes time-periodic actuation amplitudes on the prescribed control horizon  $[0, T]$ . These actuation amplitudes are optimal in the sense that they form an optimal payoff between achieving the control gain and the energy input. For the model application an overall drag reduction of 10% can be achieved. In future work optimal actuation amplitudes for more realistic flow configurations should be computed and then experimentally validated.

In the field of weakly conductive fluids open-loop optimal control with mathematical models can only serve for advancing basic research in the field. This is different for closed-loop approaches like mpc and instantaneous control. These methods combine principles of classical controller design and model based optimisation, and in future should be applied to realistic flow configurations like saltwater flow around a hydrofoil. In the model application considered in the present work instantaneous control applied to minimise the friction force on the cylinder surface yields a constant Lorentz force which may be considered as quasi-optimal in the sense that it instantaneously forms an approximately optimal payoff between achieving the control gain and the energy input.

With the present work it is shown that model based optimisation approaches applied to control weakly conductive fluids offer the potential to advance basic research in the field,

but also form a powerful mathematical tool for developing practical applicable closed-loop control mechanisms for fbws of weakly conductive fluids.

**Acknowledgements** This work is supported by the Collaborative Research Center SFB 609, sponsored by the Deutsche Forschungsgemeinschaft.

## References

- [1] Z. Chen: *Electro-Magnetic Control of Cylinder Wake*, Dissertation, New Jersey Institute of Technology, May 2001
- [2] Z. Chen, N. Aubry: *Communications in Nonlinear Science and Numerical Simulation*, 2003
- [3] T. Berger, J. Kim, C. Lee, J. Lim: *Turbulent boundary layer control utilising the Lorentz force*, *Physics of Fluids*, Vol 12 #3, March 2000, pp. 631-649
- [4] Choi, H; Temam, R.; Moin, P. and Kim, J. Feedback control for unsteady flow and its application to the stochastic Burgers equation. *J. Fluid Mech.*, 253:509 pp., 1993.
- [5] M. Gad-el-Hak: *Modern Developments in Flow Control*. In: *Appl. Mech. Rev.* 49 (1996), pp365-379
- [6] A.K. Gailitis and O.A. Lielausis: *On the possibility of drag reduction of a flat plate in an electrolyte*, *Appl. Magneto-hydrodyn.* Trudy Inst. Fiziky AN Latvia SSR 12, 143, 1961.
- [7] García, C.E.; Pretti, D.M. and Morari, M. Model predictive control: Theory and practice - a survey. *Automatica*, 25(3):335–348, 1989.
- [8] M. Hinze: *Optimal and instantaneous control of the instationary Navier-Stokes equations*, Habilitation thesis (2000), Fachbereich Mathematik, Technische Universität Berlin
- [9] M. Hinze: *Instantaneous closed-loop control of the Navier-Stokes system*, to appear in *SIAM J. Cont. Optim. Mathematik*, Technische Universität Berlin
- [10] M. Hinze, K. Kunisch: *Second order methods for optimal control of time-dependent fluid flow*, *SIAM J. Cont. Optim.* 40:925–946, 2001
- [11] M.D. Gunzburger, *Perspectives of flow control and Optimization*, Siam, 2003
- [12] P. Poncet, P. Koumoutsakos: *Proceedings of The Fourteenth International OFFSHORE AND POLAR ENGINEERING CONFERENCE*, 2004
- [13] O. Posdziech, R. Grundmann: *Electromagnetic control of seawater flow around circular cylinders*, *Eur. J. Mech. B - Fluids* 20, 2001, pp. 255-274
- [14] Rawlings, J.B. and Muske, K.R. The stability of constrained receding horizon control. *IEEE Transactions on Automatic Control*, 38(10):1512–1516, 1993.
- [15] T. Weier, G. Gerbeth, G. Mutschke, G. Platacis, O. Lielausis: *Experiments on cylinder wake stabilization in an electrolyte solution by means of electromagnetic forces localized on the cylinder surface*. *Experimental Thermal and Fluid Science* 16 (1998), pp.84-91
- [16] T. Weier, Fey, G. Gerbeth, G. Mutschke, G. Avilov: *Boundary layer control by means of electromagnetic forces*. *ERCOFTAC Bulletin* 44 2000, pp.36-40
- [17] T. Weier, J. Fey, G. Gerbeth, G. Mutschke, O. Lielausis, G. Platacis: *Boundary layer control by means of wall parallel Lorentz forces*. *Magneto-hydrodynamics* . 2001. Vol. 37, No. 1/2, pp. 177-186
- [18] T. Weier, G. Gerbeth, G. Mutschke, O. Lielausis, G. Lammers: *Control of Flow Separation Using Electromagnetic Forces*, SFB 609 Preprint 2004-03